

Transition metals in komatiitic olivine: Proxies for mantle composition, redox conditions, and sulfide mineralization potential

MAREK LOCMELIS^{1,*}, RICARDO D. AREVALO JR.², IGOR S. PUCHTEL², MARCO L. FIORENTINI³, AND EUAN G. NISBET⁴

¹Department of Geosciences and Geological and Petroleum Engineering, Missouri University of Science & Technology, Rolla, Missouri 65409, U.S.A. Orcid 0000-0002-9328-0552

²Department of Geology, University of Maryland, College Park, Maryland 20742, U.S.A.

³Centre for Exploration Targeting and ARC Centre of Excellence for Core to Crust Fluid Systems, School of Earth Sciences, The University of Western Australia, Perth WA6009, Australia

⁴Department of Earth Sciences, Royal Holloway, University of London, Egham TW20 0EX, U.K.

ABSTRACT

We present the results of a comprehensive study on the concentrations of first-row transition elements (FRTE: Sc, Ti, V, Cr, Mn, Fe, Co, Ni, Cu, and Zn), as well as Ga and Ge, in liquidus olivine from 2.7–3.5 Ga old Al-undepleted and Al-depleted komatiites from the Kaapvaal and Zimbabwe Cratons in southern Africa, the Yilgarn Craton in Australia, and the Superior Craton in Canada. The sample set includes komatiites that remained sulfur-undersaturated upon emplacement, as well as komatiites that reached sulfide saturation owing to assimilation of crustal sulfur.

All olivine grains display concentrations of Mn, Zn, Ge, Co, Fe, Mg, and Ni similar to the Bulk Silicate Earth (BSE) values, with significant negative anomalies in Sc, Ti, V, Cr, Ga, and Cu. Olivine from the studied Al-depleted komatiites displays on average higher $100\times$ Ga/Sc ratios (>5) than olivine from Al-undepleted komatiites (≤ 5). Because garnet preferentially incorporates Sc over Ga, the data suggest that elevated Ga/Sc ratios in komatiitic olivine are indicative of garnet retention in the source region of komatiites, highlighting the potential of olivine trace element chemistry as a proxy for the depth of komatiite melting and separation of the magma from the melting residue. Copper concentrations in the studied olivine grains are controlled by sulfur saturation of the host komatiite during olivine crystallization. Olivine from sulfur-undersaturated komatiite systems displays Cu concentrations mostly between 1 and 10 ppm, whereas olivine from sulfide-bearing komatiites has Cu contents of <0.5 ppm. Because komatiites contain some of the world's highest metal tenor magmatic Ni-Cu sulfide deposits, the Cu variability in olivine as a function of the sulfide-saturation state highlights a potential application of olivine chemistry in the exploration for sulfide ore deposits.

Olivine from the Paleo-Archean (3.5–3.3 Ga) komatiites displays overall higher V/Sc ratios ($V/Sc = 2.1 \pm 0.96$; 2 S.D.) than olivine from their Neo-Archean (2.7 Ga) counterparts ($V/Sc = 1.0 \pm 0.81$, 2 S.D.). Vanadium and Sc behave similarly during partial melting of the mantle and are similarly compatible in majorite garnet. However, V is redox-sensitive and its compatibility in olivine increases as the system becomes less oxidized, whereas Sc is redox-insensitive. We argue that olivine from the studied Paleo-Archean komatiites crystallized from more reduced magmas than their Neo-Archean counterparts. Elevated Fe/Mn ratios in olivine from Paleo-Archean komatiites mimic the V/Sc signatures and are interpreted to reflect that Fe^{2+} is more compatible in olivine than Fe^{3+} . These results imply that V/Sc and Fe/Mn in komatiitic olivine may potentially provide insight into the evolution of the oxidation state of the Archean mantle. Additional studies that integrate the chemistry of komatiitic olivine with those of relict interstitial glass and melt/fluid inclusions are encouraged to fully understand and quantify the potential of FRTE in olivine as a proxy for the oxidation state of the mantle sources of komatiite magmas.

Keywords: Komatiite, olivine, Archean mantle evolution, first row transition elements, oxygen fugacity, laser ablation ICP-MS

INTRODUCTION

Olivine is the most abundant mineral in the upper mantle and a major constituent of most mantle-derived rocks. However, compared to other rock-forming minerals, studies on the trace

element chemistry of olivine are underrepresented; as a result, unlocking the full potential of olivine chemistry as a petrogenetic tracer for igneous processes is a long-standing goal. An important advantage of in situ mineral analysis is that elemental signatures captured by early crystallizing minerals, such as olivine and chromite, are potentially better shielded from subsequent alteration than bulk rock signatures (e.g., Jurewicz and Watson

* E-mail: locmelism@mst.edu

1988; Foley et al. 2011; Birner et al. 2016; Locmelis et al. 2018). Therefore, the trace element chemistry of olivine may provide us with a more robust archive for early Earth processes, particularly in cases where bulk rock studies yield ambiguous results and/or sample material is limited.

Over the past two decades, most of the information on the role of olivine in the fractionation and concentration of trace elements was derived from experimental studies that focused on the partitioning of these elements between olivine and silicate melt (e.g., Canil and Fedortchouk 2001; Borisov et al. 2008; Wang and Gaetani 2008), as well as from compositional studies that investigated in situ major and minor elements by electron microprobe (e.g., Sobolev et al. 2007, 2005). However, owing to significant advances in analytical techniques, such as laser ablation-inductively coupled plasma-mass spectrometry (LA-ICP-MS) and secondary ion mass spectrometry (SIMS), there is a renewed enthusiasm on the use of olivine chemistry as a petrogenetic tracer of mantle source composition (De Hoog et al. 2010; Foley et al. 2013; Nicklas et al. 2016, 2018, 2019; Sobolev et al. 2016), in geothermometry (De Hoog et al. 2010), to track crustal recycling and interaction with carbonatitic melts (Foley et al. 2013), and as a tool in the exploration for magmatic sulfide deposits (Bulle and Layne 2015).

However, the trace element chemistry of olivine from komatiites remains largely unexplored. Here, we address this void by presenting the results of a comprehensive study of first row transition elements (FRTE = Sc, Ti, V, Cr, Mn, Fe, Co, Ni, Cu, and Zn), as well as Ga and Ge, in olivine from a globally representative sample set of 2.7 to 3.5 Ga old komatiites. Komatiites are ultramafic rocks that represent the crystallization products of magmas formed via high degrees of partial melting (up to 50%) of the mantle (Nesbitt et al. 1979; Jahn et al. 1982; Gruau et al. 1990). Because of the high MgO liquid compositions of komatiites (>18 wt% MgO anhydrous) and high liquidus temperatures (up to ~1700 °C), olivine is the only liquidus phase that crystallized in komatiites over a wide temperature interval ($\Delta T = 350$ °C) and makes up 40–80 vol% of cumulate zones of differentiated komatiite lava flows and up to 100% in adcumulus olivine dunite bodies (Arndt et al. 2008). Therefore, the compositional information extracted from komatiitic olivine can provide valuable insights into the composition of the Archean mantle, as well as on the nature of the deep melting processes that occurred during the genesis of komatiites (e.g., Nisbet et al. 1993; Sobolev et al. 2016). Furthermore, komatiites contain some of the world's highest metal tenor magmatic Ni-Cu sulfide deposits formed via sulfur saturation of komatiitic magmas and accumulation of immiscible sulfide liquid; accordingly, studies that may help constrain the

sulfide-saturation history of komatiites are of notable interest to economic geologists (e.g., Le Vaillant et al. 2016).

The FRTE, Ga, and Ge are variably siderophile and chalcophile elements that behave compatibly to mildly incompatibly during partial melting of the mantle. As a consequence, these elements have been employed as petrogenetic tracers to constrain a wide range of geochemical and physical processes. For example, the high Fe/Mn ratios recorded in basaltic lavas collected from Hawaii, Tahiti, and Reunion have been inferred to represent evidence of core-mantle exchange (e.g., Humayun et al. 2004). Furthermore, ratios of Ga/Sc (Davis et al. 2013; Le Roux et al. 2015), Ga/Ge (Arevalo and McDonough 2010), and Zn/Fe (Le Roux et al. 2010; Lee et al. 2010), as well as absolute abundances of Cu (Lee et al. 2012) and the partitioning behavior of V and Cr (Canil 1997; Delano 2001; Nicklas et al. 2016; Nicklas et al. 2018) measured in mantle-derived materials have been interpreted to reflect source lithologies and/or local redox conditions.

Here, we present the major, minor, and trace element compositions of olivine grains from a globally representative set of 2.7–3.5 Ga samples of komatiites determined by electron probe (EPMA) and laser ablation ICP-MS. The data are integrated with previously published bulk-rock data from the same locations. The results are used to discuss the usefulness of the FRTE, Ga, and Ge in olivine as petrogenetic tracers for mantle source compositions, the redox conditions of komatiite magmas, and the exploration for komatiite-hosted magmatic sulfide deposits.

SAMPLES AND GEOLOGICAL BACKGROUND

To build a globally representative suite of Archean komatiites, we analyzed well-preserved komatiites of different ages and from different cratons (Table 1), including samples from: the including samples from the 3.5 Ga Komati and 3.3 Ga Weltevreden Formations (Puchtel et al. 2013) in the Barberton greenstone belt (Kaapvaal Craton, South Africa); 2.7 Ga Tony's Flow (Bickle et al. 1993; Renner et al. 1994; Puchtel et al. 2009) in the Belingwe greenstone belt (Zimbabwe Craton, Zimbabwe); 2.7 Ga Alexo (Puchtel et al. 2004) in the Abitibi greenstone belt (Superior Craton, Canada); and 2.7 Ga Betheno (Barnes et al. 2011), Mount Clifford (Locmelis et al. 2009), Murphy Well (Locmelis et al. 2011), Perseverance (Locmelis et al. 2013), and The Horn (Locmelis et al. 2013) in the Eastern Goldfields Superterrane (Yilgarn Craton, Australia). All localities and samples are described in detail in Appendix¹ A1.

This sample selection also enables the comparison between komatiites of different geochemical affinities, i.e., Al-depleted and Al-undepleted komatiites. Aluminum-depleted komatiites

TABLE 1. Summary of localities and sample characteristics and variables included in this study

| Craton/Shield | Terrane/Belt | Locality | Age (Ga) | Affinity | Metm ^a |
|-----------------|-------------------------------------|----------------|----------|---------------|-------------------|
| Kapvaal Craton | Barberton greenstone belt | Komati | 3.5 | Al-depleted | G |
| Kapvaal Craton | Barberton greenstone belt | Weltevreden | 3.3 | Al-undepleted | G |
| Zimbabwe Craton | Belingwe greenstone belt | Tony's Flow | 2.7 | Al-undepleted | PP |
| Superior Craton | Abitibi greenstone belt | Alexo | 2.7 | Al-undepleted | PP |
| Yilgarn Craton | EGST ^b , Agnew Wiluna GB | Betheno | 2.7 | Al-undepleted | G, A |
| Yilgarn Craton | EGST, Agnew Wiluna GB | Mount Clifford | 2.7 | Al-undepleted | G, A |
| Yilgarn Craton | EGST, Agnew Wiluna GB | Perseverance | 2.7 | Al-undepleted | A |
| Yilgarn Craton | EGST, Agnew Wiluna GB | The Horn | 2.7 | Al-undepleted | G, A |
| Yilgarn Craton | EGST, Kurnalpi Terrane | Murphy Well | 2.7 | Al-undepleted | G |

^a Metamorphic grade, PP = prehnite-pumpellyite facies, G = greenschist facies, A = amphibolite facies.

^b EGST = Eastern Goldfield Superterrane.

($\text{Al}_2\text{O}_3/\text{TiO}_2 \approx 10\text{--}15$) are considered to have formed from ~30% batch melting of the mantle at depths greater than 300 km, whereby Al-depletion reflects majorite garnet retention in the mantle source and/or fractionation from the komatiite melt during magma ascent (Nesbitt et al. 1979; Jahn et al. 1982; Gruau et al. 1990). In contrast, Al-undepleted komatiites ($\text{Al}_2\text{O}_3/\text{TiO}_2 \approx 15\text{--}25$) formed from higher degrees of fractional melting (up to 50%) at depths shallower than 300 km, outside of the majorite garnet stability field. Thus, the influence of garnet retention in the source on the composition of the magma, as well as on olivine chemistry, may be interrogated through this sample set.

ANALYTICAL TECHNIQUES

Electron microprobe analyses

The major element compositions of olivine grains from Komati, Weltevreden, Tony's Flow and Alexo were determined on polished samples using a JEOL JXA-8900R electron probe microanalyzer at the Department of Geology, University of Maryland, with 15 kV accelerating potential, a 20 nA focused electron beam current, and a 10 μm spot size. Major elements (defined as >1 wt%) have been determined with an accuracy of better than 3% and an external precision of better than 3% (2 S.D.) based on replicate analyses of various probe standards. Conversely, minor elements (defined as <1 wt%) have been determined with an accuracy of better than 5% and an external precision of better than 4% (2 S.D.).

Olivine grains from Betheno, Mount Clifford, Murphy Well, Perseverance, and The Horn were analyzed using a Cameca SX-100 electron microprobe in the Geochemical Analysis Unit (GAU), GEMOC/CCFS at Macquarie University with 15 kV acceleration voltage, a 20 nA sample current and a spot size of 5 μm . Major elements have been determined with an accuracy of better than 3% and an external precision of better than 3% (2 S.D.); minor elements have been determined with an accuracy of better than 4% and an external precision of better than 4% (2 S.D.).

Laser ablation-ICP-MS analyses

The FRTE, Ga, and Ge contents of the olivine grains were determined using a Photon Machines Analyte G2 ArF Excimer laser ablation system coupled to a Nu Instruments AttoM high-resolution ICP-MS in the Planetary Environments Laboratory at NASA Goddard Space Flight Center. The analyses used 75–150 μm beam sizes, a pulse rate of 10 Hz and a constant fluence of 4.47 J/cm². The ICP-MS analyses were conducted in medium resolution mode ($M/\Delta M = 2500$, measured at 5% peak intensity) using the tunable slits offered by the Nu AttoM (Funderburg et al. 2017). Following the protocol outlined in Arevalo et al. (2011), multiple isotopes for each element (when available) were monitored to identify potential isobaric interferences, namely: ⁴⁵Sc, ^{47,49}Ti, ⁵¹V, ^{52,53}Cr, ⁵⁵Mn, ^{56,57}Fe, ⁵⁹Co, ^{60,62}Ni, ^{63,65}Cu, ^{66,67,68}Zn, ^{69,71}Ga, ^{72,73,74}Ge. Spikes in signal transients (i.e., counts-per-second vs. time), which could reflect inclusions, were excluded from the data reduction; thus, all reported elemental abundances are interpreted to reflect the matrix of the analyzed olivines. The analytical protocol and the accuracy and precision of the analyses are discussed in detail in Appendix¹ A2.

RESULTS

Bulk-rock major and minor element data

Bulk-rock data of the komatiites investigated in this study have previously been presented elsewhere (see Fig. 1 for references) and are only summarized here. All bulk-rock data have been normalized to 100% on a volatile-free basis and include the samples from this study, as well as additional samples to provide a more representative bulk-rock data set for some of the localities discussed here, i.e., Alexo, Betheno, Murphy Well, Mount Clifford, Tony's Flow samples (from the same olivine cumulate portions as the samples analyzed via LA-ICP-MS), and Weltevreden and the Komati Formation (additional flows). The bulk-rock compositions are dominantly controlled by fractionation and accumulation of olivine, resulting in olivine-controlled linear

trends of increasing $\text{FeO}_{\text{total}}$, TiO_2 , and Al_2O_3 with decreasing MgO (Figs. 1a–1c). Samples with the highest MgO abundances (49–52 wt%) are near-pure olivine cumulates (i.e., Perseverance and Betheno), whereas the lower-MgO samples are from olivine cumulate layers with lower modal olivine abundances and/or less MgO-rich olivine (e.g., 28–31 wt% MgO in Tony's Flow). Intercepts of TiO_2 and Al_2O_3 on the MgO axis are at 50–54% MgO for individual localities (Figs. 1b and 1c), implying that the bulk-rock chemistry is primarily controlled by fractionation of liquidus olivine. Nickel concentrations are typical of ultramafic systems (up to ~3000 ppm for sulfur-undersaturated komatiites with S < 0.25 wt% (Barnes 1998) and display a positive correlation with MgO (Fig. 1d). However, it is noted that some samples from Betheno are enriched in Ni (up to 7000 ppm). Conversely, samples from Mount Clifford are depleted in Ni with concentrations mostly between 800 and 1100 ppm.

Two different komatiite types can be distinguished based on their $\text{Al}_2\text{O}_3/\text{TiO}_2$ ratios and relative Al_2O_3 abundances (Fig. 1e). Komatiites from the Komati Formation have $\text{Al}_2\text{O}_3/\text{TiO}_2$ of ~10, typical of Al-depleted komatiites (Nesbitt et al. 1979; Jahn et al. 1982; Gruau et al. 1990). Samples from Tony's Flow, Alexo, Mount Clifford, and Murphy Well have average $\text{Al}_2\text{O}_3/\text{TiO}_2$ ratios of 19 to 24. These values are consistent with the Bulk Silicate Earth (BSE) $\text{Al}_2\text{O}_3/\text{TiO}_2$ ratio of 22 (McDonough and Sun 1995) and the Al-undepleted affinity of these rocks (Nesbitt et al. 1979; Jahn et al. 1982; Gruau et al. 1990). The majority of samples from Betheno, Perseverance, and The Horn have lower $\text{Al}_2\text{O}_3/\text{TiO}_2$ ratios of 4–14. However, komatiites in the Eastern Goldfield Superterrane are generally classified as Al-undepleted komatiites (Barnes 2006). The observed deviation from the typical mantle $\text{Al}_2\text{O}_3/\text{TiO}_2$ values is best explained by the very low TiO_2 concentrations, which are close to the detection limit (≤ 0.05 wt%). Samples from the Weltevreden Formation have high $\text{Al}_2\text{O}_3/\text{TiO}_2$ ratios of 28–30. However, as illustrated in Figure 1, the Al_2O_3 concentrations at a given MgO of the Weltevreden samples are identical to the Al-undepleted komatiites, whereas the high $\text{Al}_2\text{O}_3/\text{TiO}_2$ ratios are due to the lower TiO_2 contents in the former. As such, we refer to the Weltevreden komatiites as Al-undepleted.

Olivine petrography

Most olivine grains are cumulate in origin, ranging between 0.2 and 1 mm in size. Despite some replacement by serpentine around the rims and along cracks into the grains, the relict olivine cores are commonly well preserved (Figs. 2a–2c). The samples from Mount Clifford and Murphy Well are more extensively serpentinized, whereby olivine commonly occurs as rounded relict grains mostly between 100–200 μm in diameter. Although the relict olivine grains from Murphy Well are rounded, their primary skeletal texture is well preserved (Fig. 2d).

Olivine chemistry

The complete olivine data set is presented in Appendix¹ A3. All analyzed grains display similar trace element patterns when normalized to the composition of the BSE. Olivine grains from the various localities have near-BSE abundances of Mn, Zn, Ge, Co, Fe, Mg, Ni, and negative anomalies at Sc, Ti, V, Cr, Ga, and Cu (Fig. 3). The forsterite [$\text{Fo} = \text{molar Mg}/(\text{Mg}+\text{Fe}) \cdot 100$] contents of olivine are between 90 and 94, and as low as 87

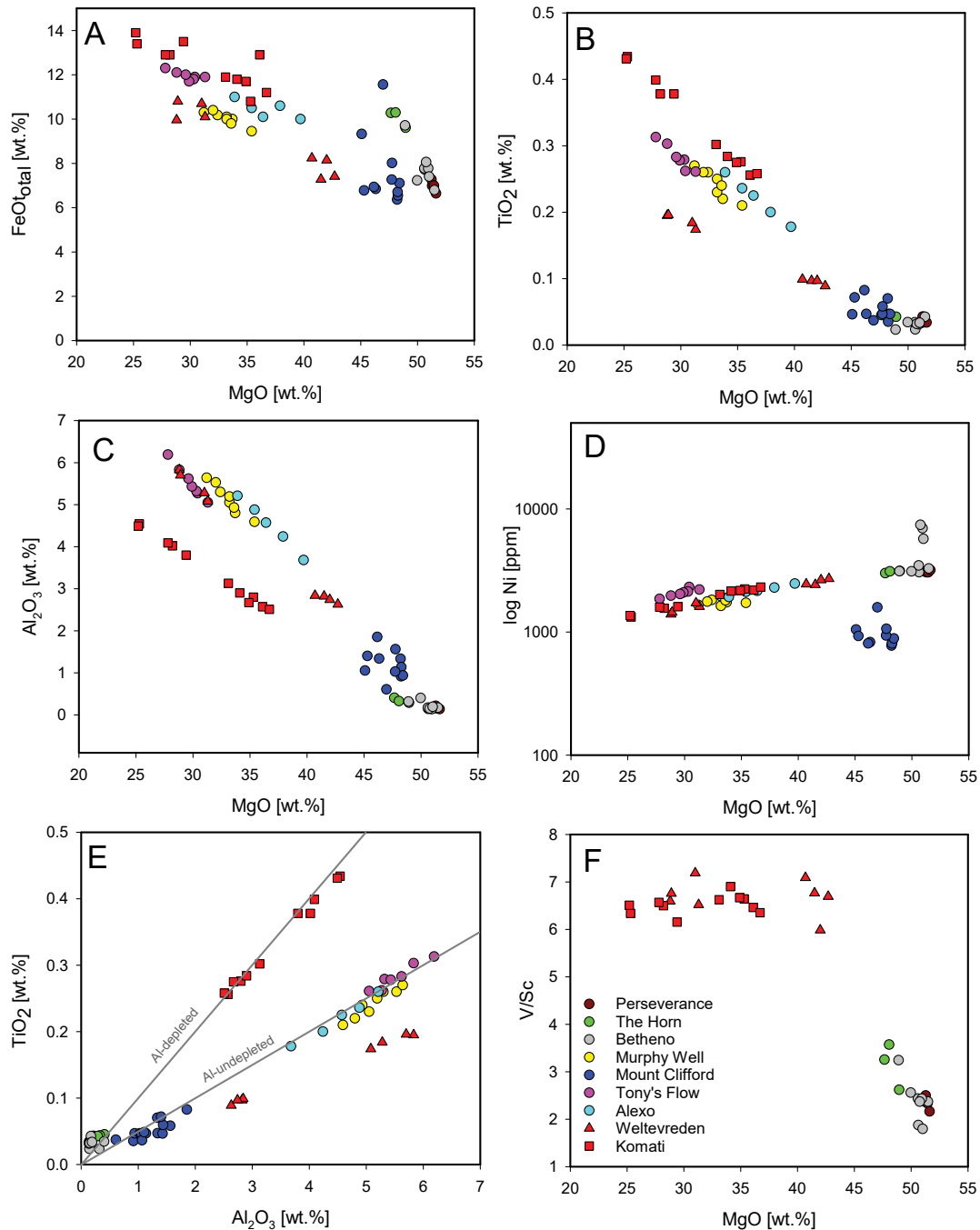


FIGURE 1. Bulk-rock chemistry of the komatiites included in this study. Data are from: Komati and Weltevreden Formations = Puchtel et al. (2013); Tony's Flow, Belingwe = Puchtel et al. (2009); Alexo, Abitibi = Puchtel et al. (2004), Mount Clifford = Locmelis et al. (2009); Betheno, Perseverance, The Horn, Murphy Well = Locmelis (2010). The symbols indicate komatiite age: circle = 2.7 Ga, ternary = 3.3 Ga, square = 3.5 Ga. The lines in **e** illustrate Al₂O₃/TiO₂ ratios representative of Al-depleted (Al₂O₃/TiO₂ = 10), and Al-undepleted (Al₂O₃/TiO₂ = 20), komatiites. (Color online.)

in one sample from Komati; olivine clusters at different Fo at Komati represent individual komatiite flows (Fig. 4; Appendix¹ A1). Grains from Weltevreden have Fo contents between 94 and 95, which are characteristic of this locality and are among the highest values reported for komatiitic olivine (Arndt et al. 2008; Puchtel et al. 2013; Byerly et al. 2017). Nickel contents are typi-

cally high (from 1900 to 4800 ppm Ni), although grains from Mount Clifford are distinctly Ni-depleted, with only 1000–1200 ppm Ni (Fig. 4a). Most olivine grains contain between 500 and 1900 ppm Cr, with no obvious correlation with Fo; grains from Betheno, Murphy Well, and Mount Clifford are notably low in Cr, with concentrations between 260 and 650 ppm Cr (Fig.

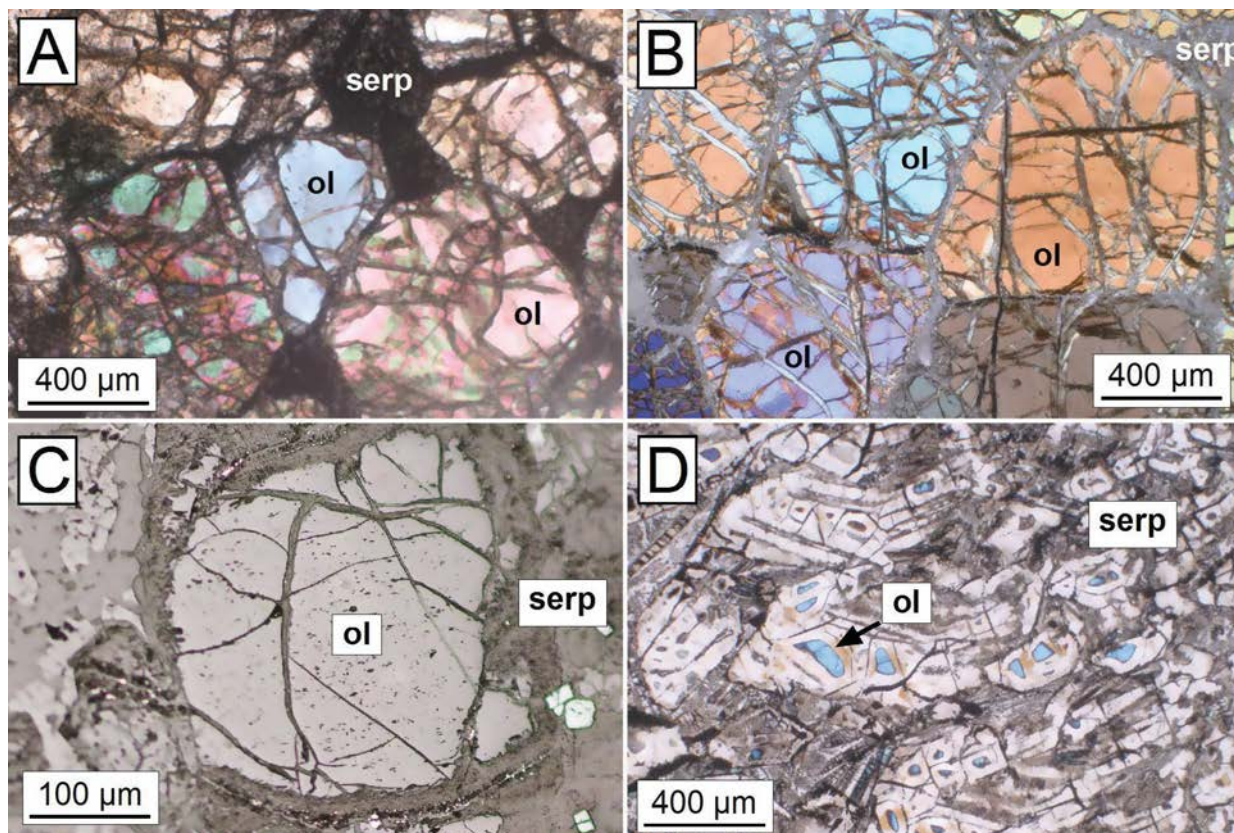


FIGURE 2. Representative images of the sample mineralogy. (a) Olivine (ol) from Betheno with interstitial serpentine (serp), sample MKT-528-352.2 (transmitted light/crossed polarizers). (b) Nearly fresh olivine from The Horn, sample LWDD-794-549.3 (transmitted light/crossed polarizers). (c) Nearly fresh olivine from Tony's Flow, sample TN-22 (scanning electron microprobe image). (d) Advanced replacement of dendritic olivine by serpentine at Murphy Well, sample MW-2303-3 (transmitted light/crossed polarizers). (Color online.)

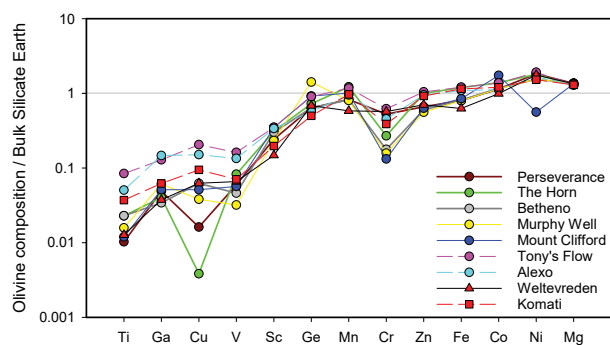


FIGURE 3. Primitive mantle-normalized concentrations of FRTE, Ga, and Ge in komatiitic olivine. The average olivine compositions for each locality are shown. Elements are ordered based on increasing olivine/melt partitioning coefficients using the recommended values of Le Roux et al. (2015) for the FRTE, Ga, and Ge, and a value of 6.6 for Mg (Kloeck and Palme 1988). Primitive mantle values are from McDonough and Sun (1995). (Color online.)

4b). Manganese displays a consistent negative correlation with Fo, with Mn contents between 550 and 1600 ppm (Fig. 4c). Negative correlations with Fo also exist for Co (90–170 ppm; 170–200 ppm at Mount Clifford), Zn (20–70 ppm), and V (1.1–11

ppm; Figs. 4d–4f, respectively), with variable degrees of scatter.

Most olivine grains contain between 6.1 and 40 ppm Ti; however, it is noted that olivine from the Komati Formation shows a distinct variability in Ti (~10–100 ppm) that is independent of Fo (Fig. 4g). Scandium ranges from 1.2 to 3.5 ppm in olivine grains from Weltevreden and the Komati Formation and from 3.0 to 6.5 ppm in all other localities (Fig. 4h). Germanium concentrations fall between 0.20 and 1.5 ppm, independently of Fo values (Fig. 4i); however, the grains from Murphy Well notably display a wide range in Ge, with concentrations between 1.0 and 3.8 ppm. Copper contents of olivine are also independent of Fo and range from 1–5 ppm in most localities, but concentrations <0.5 ppm are observed in grains from Betheno, Perseverance, and The Horn (Fig. 4j). Gallium concentrations, which range from <0.1 to 0.6 ppm, also do not correlate with Fo (Fig. 4k).

DISCUSSION

Olivine chemistry

The high Fo content of olivine (mostly between Fo 90 and 94; Fig. 4) is characteristic of olivine crystallized from primary komatiite magmas (Arndt et al. 2008). The lower Fo content of ~87 in sample BV-13 implies crystallization from a more evolved liquid. The high Ni contents of olivine between 1900 and

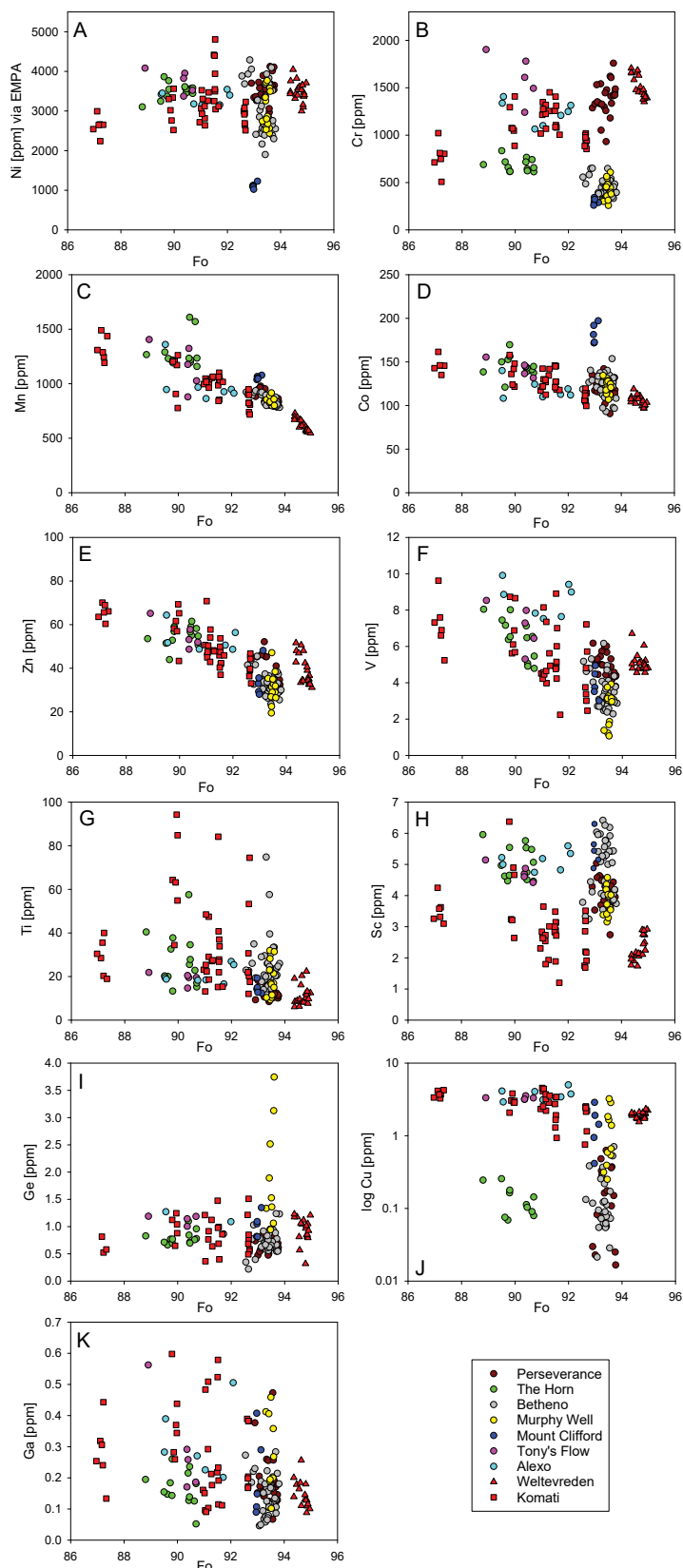


FIGURE 4. Concentrations of FRTE, Ga, and Ge in olivine vs. forsterite content.

4800 ppm and the broad positive correlation with Fo (Fig. 4b) are typical of komatiitic olivine reflecting the ultramafic nature of the komatiite magma and the compatibility of Ni in olivine (Hart and Davis 1978). The Ni depletion in grains from Mount Clifford has previously been shown to reflect early sulfide segregation that caused a Ni depletion in the magma parental to the Mount Clifford dunite (Locmelis et al. 2009). The high Cr contents of most olivine (~1000–2000 ppm Cr) are linked to high Cr concentrations in the parental melt reflecting the high degrees of partial melting that is required to form komatiite liquids; lower Cr concentrations in some samples reflect co-crystallization of minor chromite. Mn, Co, Zn and (less distinctly) V show negative correlations with Fo implying liquidus control during the fractionation of the komatiite melt (Figs. 4c–4e). The reasons for the Co enrichment in olivine from Mount Clifford (150–200 ppm Co) remain a subject of investigation. Titanium concentrations are mostly less than 70 ppm and are independent of the Fo content; such low Ti contents are typical of mantle-derived olivine (Foley et al. 2013). All other analyzed elements are discussed in the following sections.

Olivine chemistry as a proxy for mantle source composition?

Davis et al. (2013) and Le Roux et al. (2015) suggested that high bulk rock Ga/Sc ratios in mantle-derived lavas may reflect the presence of garnet in their mantle source regions; it is argued that this signature may also be recorded by early crystallizing olivine. As shown in Figure 5, 100·Ga/Sc ratios in the olivine from Al-depleted Komati Formation komatiites are on average higher than in the olivine from the Al-undepleted komatiites (all other localities). Independent and paired t-test probabilities show that the two Ga/Sc populations (i.e., Al-depleted vs. Al-undepleted types) are statistically distinct at the >95% confidence-level.

Following the argument of Davis et al. (2013) that garnet preferentially incorporates Sc over Ga ($D_{Sc}^{garnet/melt} = 6.0$; $D_{Ga}^{garnet/melt} = 0.39$), the data suggest that the elevated Ga/Sc ratios in the Komati Formation olivine reflect garnet retention in the source, corroborating the commonly accepted model for the formation of Al-depleted-type komatiites (Arndt et al. 2008). This hypothesis is strengthened by the observation that the difference in olivine Ga/Sc ratios between Al-depleted and Al-undepleted komatiites is largely driven by a depletion in Sc (Fig. 4h), whereas the Ga concentrations are similar (Fig. 4k). Such behavior is expected because Ga partitioning is largely unaffected by garnet crystallization (Davis et al. 2013). As a consequence, the results imply that olivine trace element chemistry may be successfully integrated with bulk-rock data (e.g., Al/Ti, Gd/Yb) to constrain the nature of mantle sources. However, it is

noted that the experimental data presented by Davis et al. (2013) were conducted at P - T conditions (~1.5–3.0 GPa, 1300–1500 °C) distinctly lower than the conditions expected for the source regions of Al-depleted komatiites (>10 GPa, >1700 °C; Arndt et al. 2008). Therefore, the validity of this approach remains to be experimentally tested for majorite garnet retention at higher P - T .

Arevalo and McDonough (2010) proposed that that bulk-rock Ga/Ge ratios can be used to understand the role of garnet and spinel during melting of mantle rocks, suggesting that Ga and Ge may approximate the geochemical behavior of Al and Si, respectively, but are more sensitive to geochemical processes due to their trace abundances. However, as shown in Figure 6, there are no notable differences in Ga/Ge ratios between the different komatiites, although olivine grains from Murphy Well display distinctly variable Ge contents (up to 3.8 ppm; Figs. 4i).

It is remarkable that anomalous Ge spikes were not observed during the time-resolved analyses collected in this study, suggesting that Ge does not exist as Ge-rich inclusions, but is dissolved in the olivine matrix. Although Ge concentrations are generally very low in igneous rocks and only display minor variability, significant Ge enrichments have been observed in some rocks with high volatile contents (Höll et al. 2007). This observation is noteworthy because the Murphy Well flow is considered to have crystallized from a magma with high water contents of ~3 wt% H₂O (Siégel et al. 2014). Moreover, a detailed study of early-crystallized olivine from hydrous (≥4 wt% H₂O) alkaline mantle-derived magmas emplaced in pipes in the Ivrea-Verbano Zone of northwest Italy yielded Ge concentrations similar to Murphy Well (i.e., 2–4 ppm; Locmelis et al. 2016), well above the Ge concentrations of olivine from the other komatiite localities included in this study. For comparison, the parental melt of the komatiite from Alexo has a reported water content of 0.6 wt% H₂O (Sobolev et al. 2016), whereas olivines from Belingwe crystallized from a magma with 0.2–0.3 wt% H₂O (Danyushkevsky et al. 2002; Berry et al. 2008). Because of the scarcity of published Ge data in olivine, more comprehensive studies are required to confirm if high Ge concentrations in olivine indicate crystallization from a hydrous magma, or if the observed trend is merely the result of sampling bias.

V/Sc ratios in olivine as a proxy for magma redox conditions?

The redox state of the mantle has been estimated from the partitioning behavior of V and Sc, as these elements behave in a similar way during partial melting, but V is multivalent (V²⁺ to V⁵⁺) and more compatible in olivine under reducing conditions (Canil 1997; Canil and Fedortchouk 2001; Mallmann and O'Neill 2009). In contrast, Sc is monovalent (Sc³⁺), and therefore its compatibility in olivine is not affected by shifts in oxygen fugacity (f_{O_2}) within the range observed in natural systems.

Li and Lee (2004) and Lee et al. (2005) interpreted similar bulk-rock V/Sc systematics in a global series of peridotites, mid-ocean ridge basalts, arc lavas, and ancient volcanic rocks to reflect spatial and temporal uniformity in the mantle oxidation state over the past 3.5 billion years. This conclusion is in agreement with other studies that proposed a static mantle redox

state since the Archean based on the analogous geochemical behavior of V, Cr, and Ce in contemporary and ancient magmatic materials (Canil 1997; Delano 2001; Trail et al. 2011) and Fe³⁺/ΣFe ratios measured in melt inclusions (Berry et al. 2008).

However, several more recent studies argue against static mantle redox conditions since the Archean. A more reduced Archean mantle is proposed by Aulbach and Stagno (2016) who compared V/Sc signatures of 3000–550 Ma mid-ocean ridge basalts (MORB) and picrites. Their data show that Archean suites have lower V/Sc ratios than Proterozoic and contemporary mantle-derived rocks, which these authors interpreted to reflect more reduced mantle source regions for the Archean rocks. Nicklas et al. (2018) investigated the f_{O_2} of the Archean mantle measuring the redox-sensitive partitioning of V between olivine, chromite, and komatiite melts in a series of 3.5 to 2.4 Ga komatiites. These authors speculate that a secular trend of increasing mantle f_{O_2} in the Archean exists in their data, but acknowledge that overlapping uncertainties between their data and/or with contemporary MORB lavas do not allow for a statistically robust quantification. However, a subsequent study by Nicklas et al. (2019) using a more comprehensive sample set shows compelling evidence for a secular oxidation of the Archean mantle over ~1.3 log units relative to the fayalite-magnetite-quartz buffer from 3.48 to 1.87 Ga.

In situ trace element analysis of early-formed komatiitic olivine potentially provides an alternative tool to further constrain the redox conditions of the Archean mantle. Analyses of early crystallized minerals from mantle-derived rocks have the distinct advantage that such analyses circumvent many of the uncertainties associated with bulk-rock studies, such as degassing of reduced volatiles and/or interaction with oxidizing metasomatic fluids, which may lead to the oxidation of a magma but not necessarily of its source. The hypothesis that V/Sc ratios in olivine may be indicative of magma redox conditions is supported by observations of Foley et al. (2013), who linked low V/Sc ratios (<2) in olivine from metasomatized peridotites to infiltration of oxidizing melts. Similar observations were made by Locmelis et al. (2016), who linked low V/Sc ratios (<0.5) in olivine from lower crustal alkaline ultramafic pipes in the Ivrea-Verbano Zone to their genesis through partial melting of metasomatized lithospheric mantle domains, following infiltration of oxidizing fluids and/or melts.

Here, we evaluate the applicability of V/Sc ratios in olivine as a proxy for magma redox conditions of komatiitic magmas during olivine crystallization. As shown in Figures 7a and 7b, olivine from the Paleo-Archean (3.5–3.3 Ga) komatiites have overall higher V/Sc ratios (2.1 ± 0.96; 2 S.D.) than olivine from their Neo-Archean (2.7 Ga) counterparts (V/Sc = 1.0 ± 0.81, 2 S.D.). Independent and paired t-tests show that the two V/Sc populations are statistically distinct at a >99% confidence level. A bimodal V/Sc distribution can also be seen in the bulk-rock concentrations, based on the limited published data available; i.e., Paleo-Archean samples from the Komati Formation and Weltevreden have relatively higher bulk-rock V/Sc ratios of 6.0 to 7.2, whereas Neo-Archean bulk-rock samples from Betheno, Perseverance, and The Horn are characterized by lower V/Sc = 1.8–3.6 (Fig. 1f). The V/Sc ratios observed in the bulk-rock data are overall higher than in the corresponding

olivine, suggesting that a phase other than olivine affects the total V/Sc budget of the sampled units, e.g., late magmatic chromite and/or postmagmatic alteration products. Distinguishing between different V and Sc hosts based on the published bulk-rock data is difficult, because bulk-rock signatures represent a wide range of magmatic and post-magmatic processes. This particularly applies to komatiites, where even “fresh” samples display advanced metamorphism, alteration, and/or weathering (Fig. 2), which further highlights the need for novel mineral-based petrogenetic tracers for Archean rocks. It is noted that the V/Sc ratios in olivine do not correlate with the Fo content (Fig. 7a), thereby corroborating the notion that these elements have a very similar geochemical behavior. Because V compatibility in olivine increases as the oxidation state of the system decreases, the elevated V/Sc ratios measured in the olivine grains from the Paleo-Archean systems may reflect crystallization from a more reduced magma. However, several alternative mechanisms, other than redox conditions, may be responsible for the observed V/Sc distribution. We critically discuss these alternative scenarios below.

Factors that can influence the partitioning behavior of V and Sc

(1) The partitioning of V and Sc into olivine may reflect changes in V and Sc concentrations in the coexisting melt during the crystallization of the host komatiite magma. However, according to Henry’s Law, the partitioning behavior of a trace element is independent of its concentration. Because V and Sc are trace elements in komatiites, it is unlikely that the observed V/Sc pattern reflects changes of bulk V and Sc contents in the magmas from which olivine crystallized. Increasing the concentration above a critical value may lead to concentration-dependent partitioning behavior. In such a scenario, and considering that the komatiite sequences included in this study are essentially two-component systems of olivine with accessory chromite, a concentration-dependent partitioning behavior would manifest as a distinct correlation between Fo vs. V/Sc, which is not evident in the presented data set (Fig. 7). Nonetheless, to circumvent any potential V-Sc behavioral changes related to time-varying magma composition, only the olivine cores were analyzed. Therefore, it is possible to consider the effect of evolving magma composition on V-Sc partitioning as negligible.

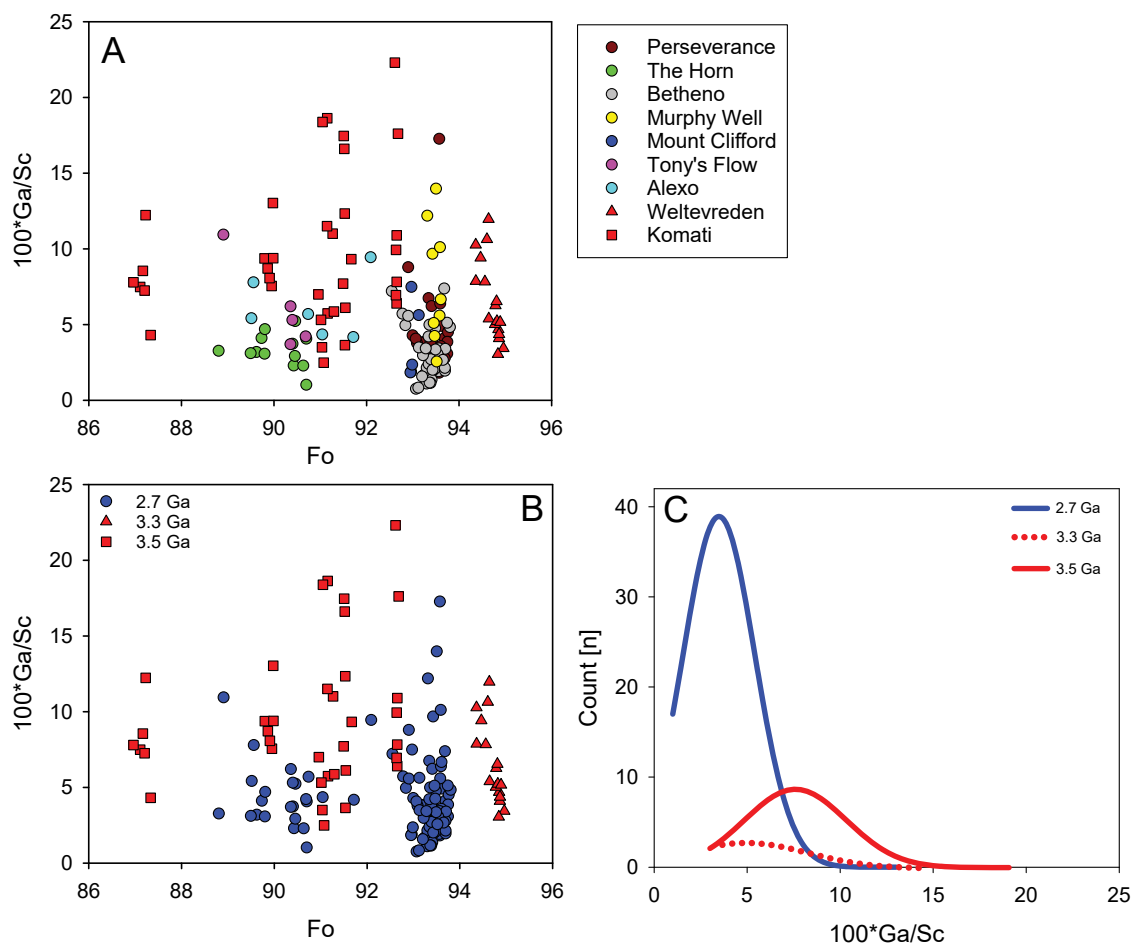


FIGURE 5. (a and b) Plots of $100^*Ga/Sc$ vs. Fo in komatiitic olivine. (c) The statistical differences between Paleo-Archean (3.3 and 3.5 Ga) and Neo-Archean (2.7 Ga) komatiites are illustrated as Gaussian distribution curves of the numerical data.

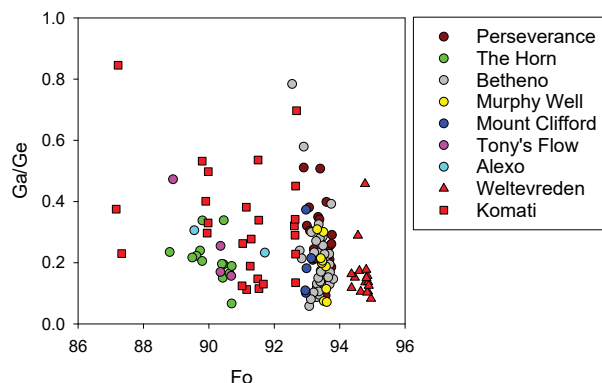


FIGURE 6. Plot of Ga/Ge vs. Fo in komatiitic olivine.

(2) The V/Sc ratios in olivine may not reflect magmatic signatures, but instead post-magmatic overprints (requiring open system behavior). However, such an assertion is improbable because bimodal distribution of V/Sc does not correlate with metamorphic grade (Table 1). Furthermore, this study only analyzed the core portions of the best preserved olivine grains in each sample. Thus, only significant mass exchange followed by complete re-equilibration of the olivine grains analyzed here could reconcile this argument, which is an unlikely scenario. This hypothesis is supported by a study of Birner et al. (2016) that shows that abyssal peridotite minerals preserve mantle f_{O_2} signatures even at high levels of alteration and/or serpentinization.

(3) The V/Sc ratios in olivine may not reflect the composition of the mantle-derived parental magma, but assimilation of sedimentary rocks upon komatiite emplacement. Thermo-mechanical erosion and assimilation of country rocks have been shown to alter the composition of komatiite magmas upon emplacement; perhaps most notably, the assimilation of crustal sulfur is required to reach sulfide saturation at low pressures and to form komatiite-hosted magmatic sulfide deposits (Leshner et al. 1984; Groves et al. 1986; Leshner 1989; Ripley et al. 1999; Bekker et al. 2009). As a consequence, it could be argued that the redox states recorded by the composition of the komatiitic olivine grains do not reflect mantle conditions, but instead the assimilation of crustal material that altered the magma composition and/or f_{O_2} . However, previous studies of lithophile element and isotope systematics have shown that crustal contamination did not play a significant role in the evolution of most of the studied komatiite systems (Puchtel et al. 2004, 2009, 2013). Localities that do show evidence of crustal assimilation through the presence of sulfides (i.e., 2.7 Ga Betheno, The Horn, and Perseverance) do not differ in terms of their olivine compositions from the other 2.7 Ga komatiites that did not assimilate enough crustal sulfur to reach sulfide saturation (Fig. 4j). Therefore, it can be argued that the olivine V/Sc contents were not notably affected by crustal assimilation.

(4) The olivine V/Sc ratios may be affected by the co-crystallization of chromite and the resulting competition for V between olivine and chromite. Although chromite grains were not analyzed for this study, several lines of evidence suggest that the effect of chromite crystallization on the V/Sc ratios of olivine is only minor. First, the absolute abundances of most major, minor,

and trace lithophile elements in the bulk komatiitic magmas (e.g., Puchtel et al. 2013), as well as in their constituent olivine (Fig. 4) track predictably with MgO, coinciding with olivine control lines as discussed above, thus suggesting that olivine was the only liquidus phase in the studied samples. Second, even if chromite would have been a liquidus phase that co-crystallized with early olivine, preferred partitioning of V into chromite only has a very limited effect on V/Sc ratios in komatiitic olivine as shown by models of fractional crystallization based on the equation of Shaw (2006):

$$C_s = F^{D-1} \cdot C_0 \cdot D \quad (2)$$

where C_s is the concentration in the crystallizing solid, F is the melt fraction, C_0 are the initial V and/or Sc contents in the source, and D is the initial bulk rock partition coefficient for V and Sc. Values for V and Sc were calculated separately. V/Sc ratios were then used to determine the amount of fractionation between V and Sc during olivine crystallization for a Fo range relevant to this study (i.e., Fo 95 to 87). Using partitioning coefficients from Mallmann and O'Neill (2009), the modeling shows that crystallization of 5% chromite causes <5% of fractionation between V and Sc at f_{O_2} conditions of QFM-0.7 to QFM+1.3 [i.e., assuming that the Neo-Archean mantle equilibrated around the QFM buffer as suggested by Canil (1997), Lee et al. (2005), and Li and Lee (2004)]. It is noted that the analyzed komatiites only contain 1–3% chromite, implying that the real effect of fractional crystallization on the V/Sc ratios in olivine is lower than the extreme case calculations assuming 5% chromite. Therefore, we argue that olivine and chromite co-crystallization cannot account for the V/Sc ratio decrease of ~50% between Paleo-Archean olivine ($V/Sc_{\text{mean}} = 2.1 \pm 0.96$; 2 S.D.) and Neo-Archean olivine ($V/Sc_{\text{mean}} = 1.0 \pm 0.81$; 2 S.D.)

(5) Some of the elevated V/Sc ratios may be due to the presence of majorite garnet in the komatiite source regions, which may have preferentially retained Sc in the residual mantle, analogous to the observations made for Ga/Sc above. As shown in Figures 7a and 7b, all Paleo-Archean komatiites are characterized by elevated V/Sc ratios, but only Komati Formation komatiites show evidence of significant garnet retained in their source. Olivine from Paleo-Archean Al-depleted (Komati: $V/Sc_{\text{mean}} = 2.0 \pm 0.92$, 2 S.D.) and Al-undepleted (Weltevreden: $V/Sc_{\text{mean}} = 2.3 \pm 0.93$, 2 S.D.) komatiites have similarly elevated V/Sc ratios, despite sampling different mantle domains and forming under different melting conditions and processes (Robin-Popieul et al. 2012). Thus, an argument can be made that V/Sc ratios can “see through” early fractional crystallization (as opposed to Ga/Sc that is indicative of garnet retention). This has previously been suggested by Li and Lee (2004) and is experimentally supported by Ohtani et al. (1989) who conducted experiments on V and Sc partition coefficients (D) between majorite garnet and ultramafic melts at high pressures (16 GPa) and temperatures (1950 °C). These authors show that the partition coefficients between majorite garnet and komatiitic melt are similar for V ($D_{V \text{ majorite/liquid}} = 1.4$) and Sc ($D_{Sc \text{ majorite/liquid}} = 1.6$), suggesting that V and Sc are not greatly fractionated via garnet retention under the conditions encountered in the source regions of komatiites. However, an argument can be made that even small differences

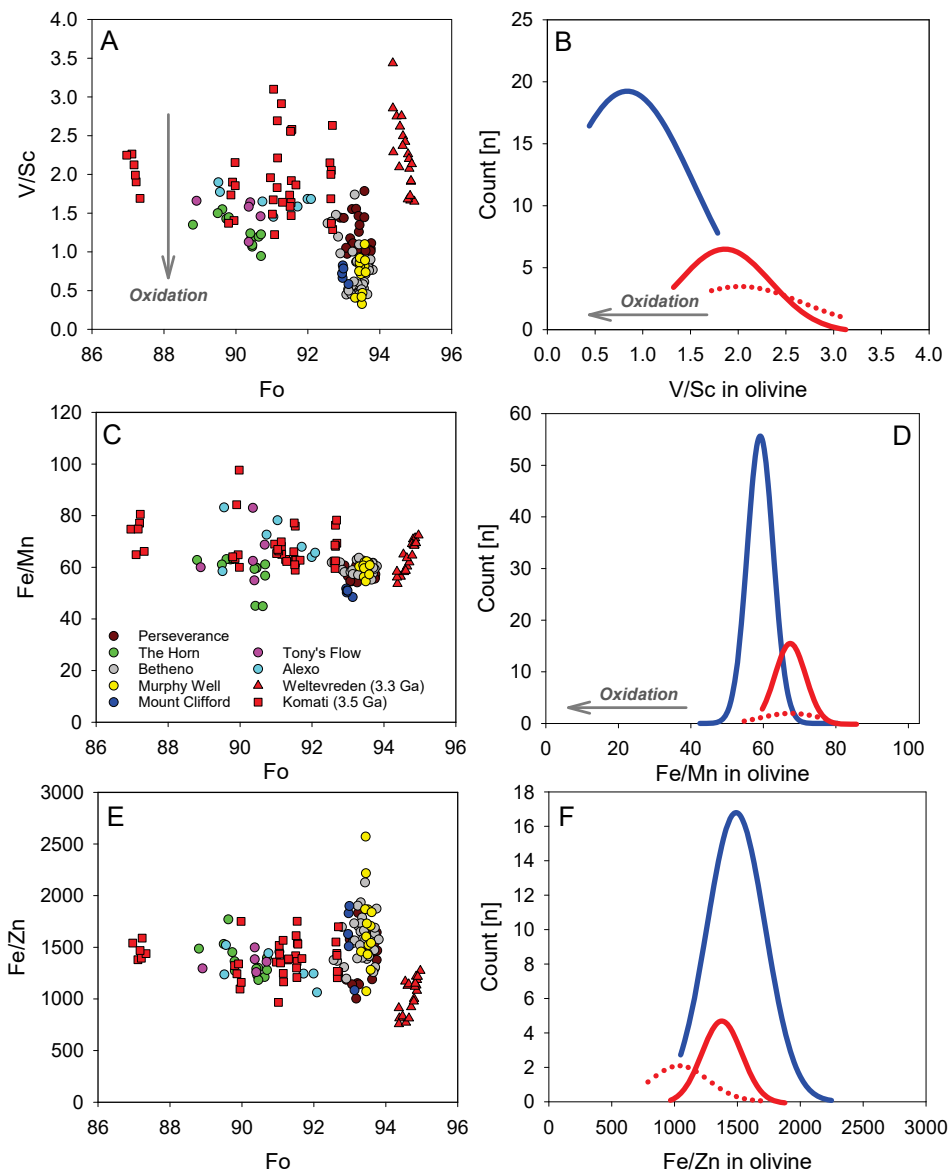


FIGURE 7. V/Sc, Fe/Mn, and Fe/Zn vs. Fo in komatiitic olivine. The statistical differences between Paleo-Archean (3.3 and 3.5 Ga) and Neo-Archean (2.7 Ga) komatiites are illustrated as Gaussian distribution curves of the numerical data on the right side.

in D_V and D_{Sc} may affect the V/Sc signatures in olivine shown in Figure 7a, particularly for Komati, which represents a mantle source that contained residual garnet. In such a scenario, the V/Sc variability shown in Figure 7a may be interpreted to primarily reflect garnet retention at Komati. Consequently, the similar V/Sc ratios observed for Paleo-Archean olivine from Weltevreten may be coincidental. Although our current data do not allow a quantification of garnet control on the V/Sc ratios measured in olivine, it is noted that the study by Nicklas et al. (2019) also observed a secular mantle oxidation in the Archean, using a similar sample set, but a redox proxy that is independent of Sc. Thus we argue that the V/Sc ratios of olivine in our presented data provide a corroborative gauge for the f_{O_2} of the komatiite magma during olivine crystallization. However, further evaluation of the

quantitative applicability of V/Sc in olivine from komatiites and more evolved systems as a proxy for magma redox conditions will require extensive studies of relict interstitial glass, and melt/fluid inclusions, as well as experimental calibration of V/Sc in olivine as an f_{O_2} meter.

In summary, the V/Sc ratios in komatiitic olivine empirically support the observations by Foley et al. (2013) and Locmelis et al. (2016) that low V/Sc ratios in olivine are indicative of oxidizing conditions during olivine crystallization. However, significant uncertainties remain regarding the usefulness of V/Sc in olivine as a reliable indicator for magma f_{O_2} . For example, even if the elevated V/Sc ratios in olivine from the 3.5 Ga Komati Formation and 3.3 Ga Weltevreten komatiites reflect crystallization from magmas that were more reduced than their 2.7 Ga counterparts, it

remains unclear if the V/Sc ratios are really indicative of a global oxidation of the Archean mantle between 3.5 and 2.7 Ga or merely reflect mantle heterogeneity. Furthermore, the variation in f_{O_2} as a function of variations in V/Sc of olivine remains to be quantified.

Sobolev et al. (2016) investigated the water content, as well as the abundances of other volatile components, in olivine from Alexo in the Abitibi greenstone belt, Canada. Their findings show that the parental melt of the Alexo komatiite was hydrous and began to crystallize under redox conditions approximately one log unit below the QFM buffer. These results are in agreement with other studies of 2.7 Ga komatiites, which demonstrated that Neo-Archean komatiites generally equilibrated at, or just below the QFM buffer (Barnes and Fiorentini 2012; Locmelis et al. 2018; Nicklas et al. 2018). Consequently, if the V/Sc ratios of olivine in Paleo-Archean komatiites reflect more reducing conditions, the Paleo-Archean mantle must have resided notably more below the QFM buffer than previously thought. This hypothesis is supported by the recent study by Nicklas et al. (2019), who propose an increase in mantle f_{O_2} of ~ 1.3 log units relative to the QFM buffer from 3.48 to 1.87 Ga based on V partitioning between liquidus olivine and komatiitic and picritic melts. The observations of this study and Nicklas et al. (2019) are intriguing, as an increase of only 0.5 log units in f_{O_2} of the mantle has been proposed as a sufficient kick-starter to instigate a transition from a reducing to an oxygenated atmosphere during the ~ 2.4 Ga Great Oxidation Event (Holland 2002).

Fe/Mn and Fe/Zn ratios in olivine: A redox proxy of the magma or a red herring?

Since the valence state of Fe ($Fe^{3+}/\Sigma Fe$) is redox sensitive, and because Fe^{2+} , Mn, and Zn behave similarly during mantle melting, Fe/Mn (Humayun et al. 2004) and Fe/Zn (Lee et al. 2010) ratios have also been used as proxies of f_{O_2} . The distribution of Fe/Mn ratios in the studied olivine grains mimics the picture portrayed by the V/Sc ratios: elevated Fe/Mn ratios in olivine from Paleo-Archean komatiites indicate more reducing conditions because Fe^{2+} is more compatible in olivine (Figs. 7c and 7d). In contrast, the distributions of Fe/Zn ratios measured in olivine from Paleo- and Neo-Archean komatiites are statistically indistinct (Figs. 7e and 7f). These conflicting findings are not surprising, as olivine-melt partitioning of Fe is less sensitive to varying f_{O_2} than V under the redox conditions typical of mantle-derived magmas, as observed in natural systems (Canil 1997; Delano 2001) and laboratory experiments (Canil and Fedortchouk 2001; Mallmann and O'Neill 2009). In addition, recent partitioning experiments indicate that Fe/Zn is a less sensitive indicator of mantle source composition than Fe/Mn (Davis et al. 2013), potentially explaining the decoupling between the Fe/Mn and Fe/Zn results.

Copper in olivine as a search criterion for magmatic sulfide ore deposits?

Komatiites contain some of the highest metal tenor magmatic Ni-Cu sulfide deposits (Barnes 2006); consequently, the development of reliable geochemical indicators to guide the search for Ni-Cu sulfide ores associated with komatiites has been a long-standing goal. Traditionally, chalcophile element abundances in bulk-rock samples were employed to determine

if a given komatiite unit reached sulfide saturation, thus making it prospective as a host for magmatic sulfide mineralization (e.g., Leshner et al. 2001; Barnes and Fiorentini 2012; Barnes et al. 2013; Le Vaillant et al. 2016). However, bulk-rock signatures represent a combined effect of several magmatic and post-magmatic processes, complicating the identification of primary ore-forming signatures. Recently, laser ablation ICP-MS studies of minerals that fingerprint magmatic sulfide ore forming processes were shown to be a powerful exploratory tool for magmatic sulfide deposits (see review by Le Vaillant et al. 2016). The data presented in this study allow further testing of the usefulness of in situ laser ablation ICP-MS as a potential triage method by comparing the trace element compositions of olivine from komatiites that host known Ni-Cu sulfide deposits to olivine grains from sulfide-undersaturated komatiites.

As shown in Figure 4j, olivine from komatiite units that host sulfide mineralization (i.e., Betheno, The Horn, and Perseverance) have significantly lower Cu concentrations than olivine from komatiites that were sulfide-undersaturated upon emplacement, although there appears to be some overlap in selected grains from the sulfide-free Murphy Well komatiite. The overall Cu variation pattern is remarkably similar to the Ru variation patterns observed for komatiitic chromite from various mineralized and barren komatiite localities (Locmelis et al. 2013, 2018) and is interpreted to reflect the competition for Cu between sulfides and olivine upon sulfide segregation. In the presence of sulfides, Cu will preferentially partition into sulfides, with sulfide-melt partition coefficients close to 1500 (Peach et al. 1990). In the absence of sulfides, Cu can more freely partition into olivine, albeit with low olivine-melt partition coefficients of < 0.15 (Lee et al. 2012; Le Roux et al. 2015). Therefore, even small amounts of sulfides in the system will strongly affect the Cu contents of olivine, providing a distinct proxy for the presence or absence of sulfides in the system.

Notably, the concentrations of other chalcophile elements in olivine, such as Ni, Zn, and Co, do not seem to be significantly influenced by the sulfide saturation state of the host komatiite magma in the studied localities, with exception of olivine from Mount Clifford that displays a strong Ni depletion. The Ni content of olivine has previously been shown to be depleted relative to typical komatiitic olivine in some magmatic sulfide ore deposits (e.g., Leshner et al. 1981; Barnes et al. 1988). However, olivine Ni depletion signatures generally appear to occur in samples that are spatially close to ore zones (Le Vaillant et al. 2016), thus hampering their usefulness in the exploration for such deposits. Zinc and Co concentrations in olivine also do not correlate with the sulfide saturation state of komatiite magmas, likely due to the fact that the partition coefficients for Zn and Co between sulfides and silicate melts are 1–2 orders of magnitude lower compared to Cu (Li and Audétat 2012). In contrast to Ni, Zn, and Co, the Cu contents of olivine appear to be distinctly more sensitive to the sulfide-saturation state. It is noted, however, that the sulfide mineralized samples included here are from large dunite bodies, whereas the non-mineralized samples are from thinner komatiite flows. It remains to be further tested if the bimodal Cu variation in olivine primarily reflects sulfide-saturation, or if it is also controlled by other factors, such as the silicate magma to sulfide melt ratio, kinetic effects

during magma emplacement and sub-solidus re-equilibration. To further develop Cu in olivine as a pathfinder for magmatic sulfide deposits, future studies will have to include olivine from thin mineralized flows, as well as large unmineralized dunite bodies.

The Cu content of olivine is also of interest as a potential redox proxy, as bulk-rock Cu in arc and mid-ocean ridge basalts has been used to reflect on mantle redox states (Lee et al. 2012). Although Cu predominantly exists as its monovalent species under the redox conditions typical of natural igneous systems, its affinity for reduced sulfide phases may be used to unravel redox conditions in mantle source regions. Based on this observation, Lee et al. (2012) interpreted identical Cu contents in primary arc and mid-ocean ridge basalts to reflect indistinguishable redox conditions between both settings. However, our data show that such an approach cannot be reliably applied to the Cu contents of olivine, as even small amounts of sulfides present in the system can potentially override any Cu-based redox signals.

IMPLICATIONS

Our study of FRTE, Ga, and Ge concentrations in olivine from a globally representative suite of komatiites measured via laser ablation ICP-MS indicates that (1) elevated Ga/Sc ratios in olivine reflect garnet retention in the komatiite source region, (2) high Ge contents in olivine may be indicative of melting under hydrous conditions in the mantle, (3) redox-sensitive V/Sc and Mn/Fe ratios in olivine can potentially be used to constrain local f_{O_2} in the komatiite magma, and (4) Cu-abundances reflect the sulfide saturation state of a komatiite magma during olivine crystallization. The results highlight that in situ trace element analysis of olivine can provide novel insight into early Earth processes, particularly in cases where bulk rock studies yield ambiguous results and/or sample material is limited.

To further evaluate the quantitative applicability of olivine trace element chemistry as a proxy for the composition and evolution of the Archean mantle, future research is encouraged to focus particularly on (1) experimental calibration of V/Sc and Mn/Fe in olivine as an f_{O_2} meter complemented by studies of relict interstitial glass and melt/fluid inclusions; and (2) systematic studies of Cu abundances in olivine from thin mineralized flows and large unmineralized dunite bodies to complement the data presented here and further test the usefulness of Cu in olivine as an exploration tool for komatiite hosted magmatic Ni-Cu sulfide deposits.

FUNDING

M.L. acknowledges support provided through a NASA-EPSCoR Missouri Research Infrastructure Development award and a University of Missouri Research Board grant. R.A.J. acknowledges funding provided through the NASA Astrobiology Institute (13-13NAI7-02-0032), NASA GSFC Science Innovation Fund, and NSF grant EAR-0739006. I.S.P. acknowledges the support from NSF FESD Type I grant no. 1338810 "The Dynamics of Earth System Oxygenation." M.L.F. acknowledges the support of the Australian Research Council through the Future Fellowship grant scheme and the Centre of Excellence for Core to Crust Fluid Systems.

ACKNOWLEDGMENTS

Bill McDonough and Steve Barnes are thanked for insightful discussions. We thank Gary Byerly for making Weltevreden komatiite samples available for this study. We thank Morris Viljoen for support and advice in the field. We also thank Richard Ash and Valentina Puchtel for contributing to the analytical methods at the University of Maryland. Will Powell is thanked for assistance with the electron microprobe analyses at Macquarie University. This paper benefited greatly from

reviews by Maryjo Brounce and Fred Davis. We thank Paul Tomascak for the editorial handling. This is a publication of the O'Keefe Institute for Sustainable Supply of Strategic Minerals at Missouri University of Science and Technology and contribution 1343 from the ARC Centre of Excellence for Core to Crust Fluid Systems (<http://www.ccfs.mq.edu.au>).

REFERENCES CITED

- Arevalo, R. Jr., and McDonough, W.F. (2010) Gallium and germanium abundances in MORB and OIB: evidence for pyroxenitic source components. *Geochimica et Cosmochimica Acta*, 74, A32–A32.
- Arevalo, R. Jr., McDonough, W.F., and Piccoli, P.M. (2011) In situ determination of first-row transition metal, Ga and Ge abundances in geological materials via medium-resolution LA-ICP-MS. *Geostandards and Geoanalytical Research*, 35, 253–273.
- Arndt, N.T., Barnes, S.J., and Leshner, C. (2008) *Komatiite*, 467 pp. Cambridge University Press, U.K.
- Aulbach, S., and Stagno, V. (2016) Evidence for a reducing Archean ambient mantle and its effects on the carbon cycle. *Geology*, 44, 751–754.
- Barnes, S.J. (1998) Chromite in komatiites, I. Magmatic controls on crystallization and composition. *Journal of Petrology*, 39, 1689–1720.
- (2006) Komatiite-hosted nickel sulfide deposits: Geology, geochemistry, and genesis. In S.J. Barnes, Ed., *Nickel Deposits of the Yilgarn Craton: Geology, Geochemistry, and Geophysics Applied to Exploration*, 13, 51–97. Society of Economic Geologists, Special Publication.
- Barnes, S.J., and Fiorentini, M.L. (2012) Komatiite magmas and sulfide nickel deposits: A comparison of variably endowed Archean terranes. *Economic Geology*, 107, 755.
- Barnes, S.J., Gole, M.J., and Hill, R.E. (1988) The Agnew nickel deposit, Western Australia: Part II, Sulfide geochemistry, with emphasis on the platinum-group elements. *Economic Geology*, 83, 537–550.
- Barnes, S.J., Godel, B.M., Locmelis, M., Fiorentini, M.L., and Ryan, C.G. (2011) Extremely Ni-rich Fe–Ni sulfide assemblages in komatiite dunite at Betheno, Western Australia: results from synchrotron X-ray fluorescence mapping. *Australian Journal of Earth Sciences*, 58, 691–709.
- Barnes, S.J., Heggie, G.J., and Fiorentini, M.L. (2013) Spatial variation in platinum group element concentrations in ore-bearing komatiite at the Long-Victor Deposit, Kambalda Dome, Western Australia: Enlarging the footprint of nickel sulfide orebodies. *Economic Geology*, 108, 913–933.
- Bekker, A., Barley, M.E., Fiorentini, M.L., Rouxel, O.J., Rumble, D., and Beresford, S.W. (2009) Atmospheric sulfur in Archean komatiite-hosted nickel deposits. *Science*, 326, 1086.
- Berry, A.J., Danyushevsky, L.V., O'Neill, H.St.C., Newville, M., and Sutton, S.R. (2008) Oxidation state of iron in komatiitic melt inclusions indicates hot Archean mantle. *Nature*, 455, 960–963.
- Bickle, M.J., Arndt, N.T., Nisbet, E.G., Orpen, J.L., Martin, A., Keays, R.R., and Renner, R. (1993) Geochemistry of the igneous rocks of the Belingwe greenstone belt: alteration, contamination and petrogenesis. *The Geology of the Belingwe Greenstone Belt, Zimbabwe*, 175–213.
- Birner, S.K., Cottrell, E., Davis, F.A., and Warren, J.M. (2016) Hydrothermal alteration of seafloor peridotites does not influence oxygen fugacity recorded by spinel oxybarometry. *Geology*, 44, 535–538.
- Borisov, A., Pack, A., Kropf, A., and Palme, H. (2008) Partitioning of Na between olivine and melt: An experimental study with application to the formation of meteoritic Na₂O-rich chondrule glass and refractory forsterite grains. *Geochimica et Cosmochimica Acta*, 72, 5558–5573.
- Bulle, F., and Layne, G.D. (2015) Trace element variations in olivine from the eastern deeps intrusion at Voisey's Bay, Labrador, as a monitor of assimilation and sulfide saturation processes. *Economic Geology*, 110, 713–731.
- Byerly, B.L., Kareem, K., Bao, H., and Byerly, G.R. (2017) Early earth mantle heterogeneity revealed by light oxygen isotopes of Archean komatiites. *Nature Geoscience*, 10, 871.
- Canil, D. (1997) Vanadium partitioning and the oxidation state of Archean komatiite magmas. *Nature*, 389, 842–845.
- Canil, D., and Fedortchouk, Y. (2001) Olivine–liquid partitioning of vanadium and other trace elements, with applications to modern and ancient picrites. *Canadian Mineralogist*, 39, 319–330.
- Danyushevsky, L.V., Gee, M.A.M., Nisbet, E.G., and Cheadle, M.J. (2002) Olivine-hosted melt inclusions in Belingwe komatiites: Implications for cooling history, parental magma composition and its H₂O content. *Geochimica et Cosmochimica Acta*, 66, A168–A168.
- Davis, F.A., Humayun, M., Hirschmann, M.M., and Cooper, R.S. (2013) Experimentally determined mineral/melt partitioning of first-row transition elements (FRTE) during partial melting of peridotite at 3 GPa. *Geochimica et Cosmochimica Acta*, 104, 232–260.
- De Hoog, J.C.M., Gall, L., and Cornell, D.H. (2010) Trace-element geochemistry of mantle olivine and application to mantle petrogenesis and geothermobarometry. *Chemical Geology*, 270, 196–215.
- Delano, J.W. (2001) Redox history of the earth's interior since ~3900 Ma: Implications for prebiotic molecules. *Origins of Life and Evolution of Biospheres*, 31, 311–341.
- Foley, S.F., Jacob, D.E., and O'Neill, H.St.C. (2011) Trace element variations in olivine phenocrysts from Ugandan potassic rocks as clues to the chemical characteristics of

- parental magmas. *Contributions to Mineralogy and Petrology*, 162, 1–20.
- Foley, S.F., Prelevic, D., Rehfeldt, T., and Jacob, D.E. (2013) Minor and trace elements in olivines as probes into early igneous and mantle melting processes. *Earth and Planetary Science Letters*, 363, 181–191.
- Funderburg, R., Arevalo, R., Locmelis, M., and Adachi, T. (2017) Improved precision and accuracy of quantification of rare earth element abundances via medium-resolution LA-ICP-MS. *Journal of The American Society for Mass Spectrometry*, 28, 2344–2351.
- Groves, D.I., Korkiakoski, E.A., McNaughton, N.J., Leshner, C.M., and Cowden, A. (1986) Thermal erosion by komatiites at Kambalda, Western Australia and the genesis of nickel ores. *Nature*, 319, 136.
- Gruau, G., Chauvel, C., Arndt, N.T., and Cornichet, J. (1990) Aluminum depletion in komatiites and garnet fractionation in the early Archean mantle: Hafnium isotopic constraints. *Geochimica et Cosmochimica Acta*, 54, 3095–3101.
- Hart, S.R., and Davis, K.E. (1978) Nickel partitioning between olivine and silicate melt. *Earth and Planetary Science Letters*, 40, 203–219.
- Höll, R., Kling, M., and Schroll, E. (2007) Metallogenesis of germanium—A review. *Ore Geology Reviews*, 30, 145–180.
- Humayun, M., Qin, L., and Norman, M.D. (2004) Geochemical evidence for excess iron in the mantle beneath Hawaii. *Science*, 306, 91–94.
- Jahn, B., Gruau, G., and Glikson, A.Y. (1982) Komatiites of the Onverwacht Group, S. Africa: REE geochemistry, Sm/Nd age and mantle evolution. *Contributions to Mineralogy and Petrology*, 80, 25–40.
- Jurewicz, A.J.G., and Watson, E.B. (1988) Cations in olivine, Part I: calcium partitioning and calcium-magnesium distribution between olivines and coexisting melts, with petrologic applications. *Contributions to Mineralogy and Petrology*, 99, 176–185.
- Kloock, W., and Palme, H. (1988) Partitioning of siderophile and chalcophile elements between sulfide, olivine, and glass in a naturally reduced basalt from Disko Island, Greenland. In G. Ryder, Ed., *Proceedings of the Lunar and Planetary Science Conference*, 18, p. 471–483. Pergamon, New York.
- Le Roux, V., Lee, C.-T.A., and Turner, S.J. (2010) Zn/Fe systematics in mafic and ultramafic systems: Implications for detecting major element heterogeneities in the Earth's mantle. *Geochimica et Cosmochimica Acta*, 74, 2779–2796.
- Le Roux, V., Dasgupta, R., and Lee, C.-T.A. (2015) Recommended mineral-melt partition coefficients for FRTes (Cu, Ga, and Ge during mantle melting. *American Mineralogist*, 100, 2533–2544.
- Le Vaillant, M., Fiorentini, M.L., and Barnes, S.J. (2016) Review of lithochemical exploration tools for komatiite-hosted Ni-Cu-(PGE) deposits. *Journal of Geochemical Exploration*, 168, 1–19.
- Lee, C.-T.A., Leeman, W.P., Canil, D., and Li, Z.X.A. (2005) Similar V/Sc systematics in MORB and arc basalts: implications for the oxygen fugacities of their mantle source regions. *Journal of Petrology*, 46, 2313–2336.
- Lee, C.-T.A., Luffi, P., Le Roux, V., Dasgupta, R., Albarede, F., and Leeman, W.P. (2010) The redox state of arc mantle using Zn/Fe systematics. *Nature*, 468, 681–685.
- Lee, C.-T.A., Luffi, P., Chin, E.J., Bouchet, R., Dasgupta, R., Morton, D.M., Le Roux, V., Yin, Q.-Z., and Jin, D. (2012) Copper systematics in arc magmas and implications for crust-mantle differentiation. *Science*, 336, 64–68.
- Leshner, M.C. (1989) Komatiite-associated nickel sulfide deposits. *Reviews in Economic Geology*, 4, 44–101.
- Leshner, C.M., Lee, R.F., Groves, D.I., Bickle, M.J., and Donaldson, M.J. (1981) Geochemistry of komatiites from Kambalda, Western Australia; I. Chalcophile element depletion, a consequence of sulfide liquid separation from komatiitic magmas. *Economic Geology*, 76, 1714–1728.
- Leshner, C.M., Arndt, N.T., and Groves, D.I. (1984) Genesis of komatiite-associated nickel sulfide deposits at Kambalda Western Australia: a distal volcanic model. In D.L. Buchanan and M.J. Jones, Eds., *Sulfide Deposits in Mafic and Ultramafic Rocks*, 70–80. Institute of Mining and Metallurgy, London.
- Leshner, C.M., Burnham, O.M., Keays, R.R., Barnes, S.J., and Hulbert, L. (2001) Trace-element geochemistry and petrogenesis of barren and ore-associated komatiites. *Canadian Mineralogist*, 39, 673–696.
- Li, Y., and Audétat, A. (2012) Partitioning of V, Mn, Co, Ni, Cu, Zn, As, Mo, Ag, Sn, Sb, W, Au, Pb, and Bi between sulfide phases and hydrous basanite melt at upper mantle conditions. *Earth and Planetary Science Letters*, 355–356, 327–340.
- Li, Z.-X.A., and Lee, C.-T.A. (2004) The constancy of upper mantle f_{O_2} through time inferred from V/Sc ratios in basalts. *Earth and Planetary Science Letters*, 228, 483–493.
- Locmelis, M. (2010) Mechanisms of platinum-group element fractionation in ultramafic melts and implications for the exploration for magmatic nickel-sulphide deposits. Ph.D. thesis, Macquarie University, Sydney, Australia, 241pp.
- Locmelis, M., Barnes, S.J., Pearson, N.J., and Fiorentini, M.L. (2009) Anomalous Sulfur-Poor Platinum Group Element Mineralization in Komatiitic Cumulates, Mount Clifford, Western Australia. *Economic Geology*, 104, 841–855.
- Locmelis, M., Pearson, N.J., Barnes, S.J., and Fiorentini, M.L. (2011) Ruthenium in komatiitic chromite. *Geochimica et Cosmochimica Acta*, 75, 3645–3661.
- Locmelis, M., Fiorentini, M.L., Barnes, S.J., and Pearson, N.J. (2013) Ruthenium variation in chromite from komatiites and komatiitic basalts—A potential mineralogical indicator for nickel sulfide mineralization. *Economic Geology*, 108, 355–364.
- Locmelis, M., Fiorentini, M.L., Rushmer, T., Arevalo, R. Jr., Adam, J., and Denyszyn, S.W. (2016) Sulfur and metal fertilization of the lower continental crust. *Lithos*, 244, 74–93.
- Locmelis, M., Fiorentini, M.L., Barnes, S.J., Hanski, E.J., and Kobussen, A.F. (2018) Ruthenium in chromite as indicator for magmatic sulfide liquid equilibration in mafic-ultramafic systems. *Ore Geology Reviews*, 97, 152–170.
- Mallmann, G., and O'Neill, H.St.C. (2009) The Crystal/Melt Partitioning of V during Mantle Melting as a Function of Oxygen Fugacity Compared with some other Elements (Al, P, Ca, Sc, Ti, Cr, Fe, Ga, Y, Zr and Nb). *Journal of Petrology*, 50, 1765–1794.
- McDonough, W.F., and Sun, S.-S. (1995) The composition of the Earth. *Chemical Geology*, 120, 223–253.
- Nesbitt, R.W., Sun, S.S., and Purvis, A.C. (1979) Komatiites: geochemistry and genesis. *Canadian Mineralogist*, 17, 165–186.
- Nicklas, R.W., Puchtel, I.S., and Ash, R.D. (2016) High-precision determination of the oxidation state of komatiite lavas using vanadium liquid-mineral partitioning. *Chemical Geology*, 433, 36–45.
- (2018) Redox state of the Archean mantle: Evidence from V partitioning in 3.5–2.4 Ga komatiites. *Geochimica et Cosmochimica Acta*, 222, 447–466.
- Nicklas, R.W., Puchtel, I.S., Ash, R.D., Piccoli, P.M., Hanski, E., Nisbet, E.G., Waterton, P., Pearson, D.G., and Anbar, A.D. (2019) Secular mantle oxidation across the Archean-Proterozoic boundary: Evidence from V partitioning in komatiites and picrites. *Geochimica et Cosmochimica Acta*, 250, 49–75.
- Nisbet, E.G., Cheadle, M.J., Arndt, N.T., and Bickle, M.J. (1993) Constraining the potential temperature of the Archean mantle: A review of the evidence from komatiites. *Lithos*, 30, 291–307.
- Ohtani, E., Kawabe, I., Moriyama, J., and Nagata, Y. (1989) Partitioning of elements between majorite garnet and melt and implications for petrogenesis of komatiite. *Contributions to Mineralogy and Petrology*, 103, 263–269.
- Peach, C.L., Mathez, E.A., and Keays, R.R. (1990) Sulfide melt-silicate melt distribution coefficients for noble metals and other chalcophile elements as deduced from MORB: Implications for partial melting. *Geochimica et Cosmochimica Acta*, 54, 3379–3389.
- Puchtel, I.S., Humayun, M., Campbell, A.J., Sproule, R.A., and Leshner, C.M. (2004) Platinum group element chemistry of komatiites from the Alexo and Pyke Hill areas, Ontario, Canada. *Geochimica et Cosmochimica Acta*, 68, 1361–1383.
- Puchtel, I.S., Walker, R.J., Brandon, A.D., and Nisbet, E.G. (2009) Pt–Re–Os and Sm–Nd isotope and HSE and REE systematics of the 2.7 Ga Belingwe and Abitibi komatiites. *Geochimica et Cosmochimica Acta*, 73, 6367–6389.
- Puchtel, I.S., Blichert-Toft, J., Touboul, M., Walker, R.J., Byerly, G.R., Nisbet, E.G., and Anhaeusser, C.R. (2013) Insights into early Earth from Barberton komatiites: Evidence from lithophile isotope and trace element systematics. *Geochimica et Cosmochimica Acta*, 108, 63–90.
- Renner, R., Nisbet, E.G., Cheadle, M.J., Arndt, N.T., Bickle, M.J., and Cameron, W.E. (1994) Komatiite flows from the reliance formation, Belingwe Belt, Zimbabwe: I. Petrography and mineralogy. *Journal of Petrology*, 35, 361–400.
- Ripley, E.M., Park, Y.-R., Li, C., and Naldrett, A.J. (1999) Sulfur and oxygen isotopic evidence of country rock contamination in the Voisey's Bay Ni–Cu–Co deposit, Labrador, Canada. *Lithos*, 47, 53–68.
- Robin-Popieul, C.C.M., Arndt, N.T., Chauvel, C., Byerly, G.R., Sobolev, A.V., and Wilson, A. (2012) A new model for Barberton komatiites: Deep critical melting with high melt retention. *Journal of Petrology*, 53, 2191–2229.
- Shaw, D.M. (2006) *Trace Elements in Magmas: A theoretical treatment*. Cambridge University Press, U.K., 243pp.
- Siégl, C., Arndt, N., Barnes, S.J., Henriot, A.-L., Haenecour, P., Debaille, V., and Mattioli, N. (2014) Fred's Flow (Canada) and Murphy Well (Australia): thick komatiitic lava flows with contrasting compositions, emplacement mechanisms and water contents. *Contributions to Mineralogy and Petrology*, 168, 1–17.
- Sobolev, A.V., Hofmann, A.W., Sobolev, S.V., and Nikogosian, I.K. (2005) An olivine-free mantle source of Hawaiian shield basalts. *Nature*, 434, 590–597.
- Sobolev, A.V., Hofmann, A.W., Kuzmin, D.V., Yaxley, G.M., Arndt, N.T., Chung, S.-L., Danyushevsky, L.V., Elliott, T., Frey, F.A., Garcia, M.O., and others. (2007) The amount of recycled crust in sources of mantle-derived melts. *Science*, 316, 412.
- Sobolev, A.V., Asafov, E.V., Gurenko, A.A., Arndt, N.T., Batanova, V.G., Portnyagin, M.V., Garbe-Schönberg, D., and Krashennnikov, S.P. (2016) Komatiites reveal a hydrous Archean deep-mantle reservoir. *Nature*, 531, 628–632.
- Trail, D., Watson, B.E., and Tailby, N.D. (2011) The oxidation state of Hadean magmas and implications for early Earth's atmosphere. *Nature*, 480, 79–82.
- Wang, Z., and Gaetani, G.A. (2008) Partitioning of Ni between olivine and siliceous eclogite partial melt: experimental constraints on the mantle source of Hawaiian basalts. *Contributions to Mineralogy and Petrology*, 156, 661–678.

MANUSCRIPT RECEIVED NOVEMBER 30, 2018
 MANUSCRIPT ACCEPTED APRIL 9, 2019
 MANUSCRIPT HANDLED BY PAUL TOMASCAK

Endnote:

¹Deposit item AM-19-86914, Supplemental Material. Deposit items are free to all readers and found on the MSA website, via the specific issue's Table of Contents (go to http://www.minsocam.org/MSA/AmMin/TOC/2019/Aug2019_data/Aug2019_data.html).